



| | |
|------------------------|--|
| Title | The solid-phase partitioning of arsenic in unconsolidated sediments of the Mekong Delta, Vietnam and its modes of release under various conditions |
| Author(s) | Dang Thuong Huyen; Tabelin, Carlito Baltazar; Huynh Minh Thuan; Dang Hai Dang; Phan Thi Truong; Vongphuthone, Banthasith; Kobayashi, Masato; Igarashi, Toshifumi |
| Citation | Chemosphere, 233, 512-523 https://doi.org/10.1016/j.chemosphere.2019.05.235 |
| Issue Date | 2019-10 |
| Doc URL | http://hdl.handle.net/2115/82845 |
| Rights | © 2019. This manuscript version is made available under the CC-BY-NC-ND 4.0 license https://creativecommons.org/licenses/by-nc-nd/4.0/ |
| Rights(URL) | https://creativecommons.org/licenses/by-nc-nd/4.0/ |
| Type | article (author version) |
| Additional Information | There are other files related to this item in HUSCAP. Check the above URL. |
| File Information | Manuscript (Chemosphere-revision 1).pdf |



[Instructions for use](#)

1 **The solid-phase partitioning of arsenic in unconsolidated sediments of the Mekong**
2 **Delta, Vietnam and its modes of release under various conditions**

3 Dang Thuong Huyen^a, Carlito Baltazar Tabelin^{b,*}, Huynh Minh Thuan^a, Dang Hai Dang^a, Phan Thi
4 Truong^a, Banthasith Vongphuthone^c, Masato Kobayashi^c, and Toshifumi Igarashi^d

5
6 ^aEnvironmental Geology Department, Faculty of Geology and Petroleum Engineering, Ho Chi Minh City
7 University of Technology, 168 Ly Thuong Kiet, Dist. 10, HCMC, VIETNAM

8 ^bSchool of Minerals and Energy Resources Engineering, The University of New South Wales, Sydney, NSW
9 2052, AUSTRALIA

10 ^cDivision of Sustainable Resources Engineering, Graduate School of Engineering, Hokkaido University, JAPAN

11 ^dDivision of Sustainable Resources Engineering, Faculty of Engineering, Hokkaido University, JAPAN

12
13 **Abstract**

14 Arsenic (As) contamination of the groundwater in the Mekong Delta is a serious problem affecting
15 millions of people who rely on this important resource for drinking and agriculture. In this study,
16 borehole cores up to a depth of 40 m were collected in the Vietnamese-side of the delta and the solid-
17 phase partitioning of As with depth was investigated to understand the factors and processes
18 controlling its release under oxic, acidic and reducing conditions. The results showed that in most of
19 the sediments, substantial amounts of As are partitioned with exchangeable phases that are easily
20 released into solution. Two borehole cores obtained between the Hau and Tien Rivers also had
21 significantly high As partitioned with organic/sulfide phases and one of these cores had abundant As-
22 bearing pyrite in 1-m thick peat layers. Leaching experiments in deionized (DI) water coupled with
23 principal component analysis suggest that As release is controlled by sorption-desorption reactions
24 with clays/phyllosilicates (i.e., kaolinite, muscovite and clinochlore), proton-promoted dissolution of
25 iron-oxyhydroxides, and oxidation of pyrite/organic matter. The release of As was further promoted
26 under acidic conditions in the presence of chloride (Cl⁻), which suggests that seasonal drying/flooding
27 episodes generating acid sulfate soils, as well as salt water intrusion due to excessive groundwater
28 abstraction may exacerbate this problem in the future.

29
30 *Keywords: Vietnamese Mekong Delta; arsenic; leaching; sequential extraction; pyrite; phyllosilicates*

*Corresponding author: Tel: +61 (02) 9385 7946

Email: c.tabelin@unsw.edu.au; carlito.tabelin@gmail.com

31 **1. INTRODUCTION**

32 Groundwater contaminated with arsenic (As) is one of the biggest and most serious health threats in
33 developing countries because it is almost always used directly without prior treatment (Smedley and
34 Kinniburgh, 2002). Arsenic is a metalloid with mutagenic, carcinogenic and teratogenic properties,
35 and prolonged exposure to it even in minute amounts (i.e., chronic poisoning) via ingestion of
36 contaminated drinking water could cause arsenicosis, Blackfoot disease and the higher risks of
37 developing various types of cancers (Tabelin et al., 2018). To date, As-contaminated groundwater has
38 been reported in over 70 countries and is affecting more than 150 million people worldwide
39 (Ravenscroft et al., 2009).

40 The Mekong Delta, situated in Cambodia and Vietnam, is an important aquifer system with
41 prevalent and serious As-contaminated groundwater problem. The delta plain was formed as the
42 Mekong River breaks into several arteries before reaching the sea and has an area of around 62 000
43 km² with about 84% of it situated in Vietnam while the rest is in Cambodia (~16%) (Nguyen et al.,
44 2000). Arsenic contamination of groundwater in the Mekong Delta was first reported in 2001 by a
45 study conducted in Cambodia (Feldman and Rosenboom, 2001). Six years later, Berg and coworkers
46 (2007) reported that groundwater in the Vietnamese-side of the Mekong Delta was also contaminated
47 with As. They further estimated that more than 17 million Vietnamese living on the delta is highly at
48 risk of chronic As poisoning. In fact, the hairs of some affected Vietnamese already had elevated As
49 levels, an early symptom of chronic As poisoning (Berg et al., 2007). With the rapid population
50 increase in this region coupled with the extensive use of groundwater for drinking and agriculture, this
51 As-contaminated groundwater problem will likely worsen as observed in other parts of the world like
52 Bangladesh and West Bengal, India with high population densities (Fendorf et al., 2010; Harvey et al.,
53 2002).

54 The geological, hydrological and biological processes crucial in the release of As to
55 groundwater as well as its migration through aquifer systems are increasingly becoming well defined
56 in recent years. Polizzotto and coworkers (2008), for example, studied in detail how hydrological and
57 biogeochemical conditions affected As fluxes in a minimally disturbed area of the Mekong Delta in
58 Kandal Province, Cambodia and found that wetlands and near-surface sediments supplied As to lower

59 regions of the aquifer. A follow-up paper by these authors proposed that organic matter from wetlands
60 was likely co-deposited with As-bearing iron-oxyhydroxides and as these phases moved downwards
61 into the aquifer during burial, microbial-mediated processes driven by organic matter decomposition
62 promoted reducing conditions that remobilized As into groundwater in the deeper parts of the aquifer
63 (Kocar et al., 2008). These studies were, however, limited in Cambodia and the area selected had a
64 relatively simple vertical lithofacies composed mainly of an upper layer of clay and a lower layer of
65 sand. Moreover, these studies only determined the solid-phase partitioning of As in a very shallow part
66 of the aquifer (about 4 m from the surface). On the Vietnamese-side of the Mekong Delta, only the
67 work of Hoang and coworkers (2010) evaluated the solid-phase partitioning of As in the sediments by
68 sequential extraction using sections from two borehole cores. These authors provided compelling
69 evidence that As concentration in groundwater tended to increase when the wells are closer to the Tien
70 River, one of the main arteries of the Mekong River in Vietnam. Moreover, they reported that
71 amorphous iron-oxyhydroxides were the primary sources of As in the sediments. Unfortunately, these
72 authors ignored the effects of pyrite/organic matter and clay/phyllsilicate minerals likely because the
73 sequential extraction method they employed was designed to quantify As in both amorphous and
74 crystalline iron-oxyhydroxide/oxide phases (Silveira et al., 2006). In other words, the solid-phase
75 partitioning of As in the sediments of the Mekong Delta still remains unclear.

76 Another important issue that is still not well understood is how the seasonal changes in aquifer
77 conditions (i.e., oxidizing-reducing and acidification) affect the mobility of As in the sediments of the
78 Mekong Delta. The climate in this region is monsoonal humid and tropical (27–30°C) with a mean
79 annual precipitation of 1500–2400 mm, the bulk of which is delivered during the rainy season from
80 April to November (Pham et al., 2002). These seasonal cycles of dry and wet conditions have been
81 reported to strongly affect redox conditions in the shallow regions of the Mekong Delta including
82 areas near the Mekong River and its tributaries (Polizotto et al., 2008). Meanwhile, the abundance of
83 acid sulfate soils in the region suggests that acidification of sediments in the aquifer could occur as a
84 result of hydrological changes caused by excessive groundwater abstraction or flooding/inundation
85 episodes due to the delta's low elevation (0–4 m above sea level) (Berg et al., 2007; Nguyen and Itoi,
86 2009).

87 The above-mentioned issues are addressed in this study by providing a better understanding of
88 the solid-phase partitioning of As in naturally contaminated aquifer sediments and the roles played by
89 these As-bearing phases on the release of As under oxic, reducing and acidic conditions. Specifically,
90 this study aims to: (1) determine the solid-phase partitioning of As with depth in the upper region (<
91 40 m) of the Vietnamese-side of the Mekong Delta, (2) investigate the effects of oxic, reducing and
92 acidic conditions on the release of As into solution, and (3) identify the important factors and
93 processes responsible for the mobilization/immobilization of As under various environmentally
94 relevant conditions. The first objective was achieved by extensive characterization of the sediments
95 using X-ray powder diffraction (XRD), X-ray fluorescence spectroscopy (XRF), scanning electron
96 microscopy with energy dispersive X-ray spectroscopy (SEM-EDX) and sequential extraction. The
97 second and third objectives were accomplished by batch-type leaching experiments under oxic,
98 reducing and acidic conditions supplemented by multivariate statistical analysis and geochemical
99 modeling.

100 **2. MATERIALS AND METHODS**

101 2.1 Borehole core sampling and characterization of sediments

102 The Mekong River breaks into two main arteries, the Tien and Hau Rivers, as it enters Vietnam and
103 further branches out into eight smaller Rivers before reaching the sea (Hoang et al., 2010). The
104 Vietnamese-side of the Mekong delta covers an area of around 39 200 km² and is composed of
105 Holocene alluvial sediments (depths of 8–40 m) overlying late Pleistocene sediments (50–80 m) (Bui
106 et al., 2005). Six borehole cores were drilled with depths of 20–40 m near the two main arteries of the
107 Mekong River in Vietnam: two along the Hau River (PH and P-Hu), two near the Tien River (TT and
108 TL), and two adjacent to river tributaries between the Hau and Tien Rivers (LS and PT) (Fig. 1). A
109 total of 34 samples were obtained from distinct lithological features of the six borehole cores and a
110 brief description of each sample is summarized in Supplementary Table 1. The samples were air-dried
111 in the laboratory, sealed in polypropylene (PP) bottles, and then shipped to Hokkaido University,
112 Japan for the detailed characterization of the sediments, leaching experiments and sequential
113 extraction.

114 Prior to the chemical and mineralogical analyses, the samples were ground with an agate
115 mortar to $< 50 \mu\text{m}$ and then analyzed by XRD (MultiFlex, Rigaku Corporation, Japan) and XRF
116 (SpectroXepos, Rigaku Corporation, Japan). Both XRD and XRF measurements were done on pressed
117 powders of the samples. All 34 XRD patterns were also analyzed using Match!® (Crystal Impact,
118 Germany) to identify minerals and semi-quantitatively determine their relative abundances in the
119 samples. Loss on ignition (LOI) was determined by gravimetry; that is, a known amount of sample
120 was heated in a muffle furnace at 750°C for 1 h after drying at 110°C in an oven for 24 h, and its loss
121 in mass corresponded to LOI. Total organic carbon (TOC) was calculated from the total carbon (TC)
122 and inorganic carbon (IC) contents of the sediments, both of which were measured using a total carbon
123 analyzer attached to a solid sample combustion unit (TOC-V_{CSH}-SSM-5000A, Shimadzu Corporation,
124 Japan). Selected samples that have exceptionally high As were also examined using SEM-EDX
125 (Superscan SSX-550, Shimadzu Corporation, Japan).

126 The sequential extraction procedure used in this study was developed by Marumo and
127 coworkers (2003) for contaminated soils and sediments based on the earlier works of Tessier et al.
128 (1979) and Clevenger (1990). This procedure involves the sequential leaching of 1 g of sample with
129 various lixiviants to target specific As-bearing phases. The extracted phases, lixiviants and conditions
130 used in each extraction step are detailed as follows:

- 131 • Step 1 (exchangeable): 1 M sodium dihydrogen phosphate (NaH_2PO_4) (pH 5; 1 h; liquid-to-
132 solid ratio of 20; 25°C ; 120 rpm),
- 133 • Step 2 (carbonates): 1 M sodium acetate (CH_3COONa) (pH 5; 5 h; liquid-to-solid ratio of 20;
134 25°C ; 120 rpm),
- 135 • Step 3 (Fe-Mn oxides): 0.04M $\text{NH}_2\text{OH}\cdot\text{HCl}$ in 25% acetic acid (5 h; liquid-to-solid ratio of
136 20; 80°C ; 120 rpm), and
- 137 • Step 4 (organic and sulfides): 0.04M $\text{NH}_2\text{OH}\cdot\text{HCl}$ in 25% acetic acid + 30% H_2O_2 + 0.02 M
138 HNO_3 (5 h; liquid-to-solid ratio of 36; 80°C ; 120 rpm).

139 The residue from each extraction step was washed with 10–15 ml DI water and this solution was
140 combined with the leachate of the extraction step and diluted to 50 ml. Finally, the residual fraction

141 was calculated by subtracting the total As extracted by the four steps to the As content of the sample
142 measured by XRF.

143 2.2 Batch-type leaching experiments

144 Three types of batch-type leaching experiments were conducted in this study using a particle size of <
145 2 mm. Under oxic conditions, As release was evaluated by leaching 15 g of sediment samples with
146 150 ml of DI water at 200 rpm for 6 h using a reciprocal shaker. This method was based on the
147 standard Japanese leaching test for contaminated soils (Environmental Agency of Japan Notification
148 No. 46) (Tabelin et al., 2014a). After 6 h, the temperature, pH, redox potential (Eh) and electrical
149 conductivity (EC) of suspensions were measured. Separation of liquid (supernatant) and solid
150 (residue) was done by centrifugation for 30 min at 3500 rpm and the supernatant was filtered through
151 0.45 µm Millex® membrane filters (Merck Millipore, USA). The leaching experiments under
152 reducing conditions were conducted using sodium dithionite ($\text{Na}_2\text{S}_2\text{O}_4$) as a reducing agent. Five
153 grams of the sample (< 2 mm) were mixed with 50 ml of 0.1 M $\text{Na}_2\text{S}_2\text{O}_4$ solution at 200 rpm in a
154 sealed 50-ml centrifuge tube to minimize the oxidation of $\text{S}_2\text{O}_4^{2-}$. After 6 h, the temperature, pH and
155 Eh were measured and the leachates were then collected by filtration through 0.45 µm Millex®
156 membrane filters. The leaching experiments under acidic conditions were done using hydrochloric
157 acid (HCl) solutions. In these experiments, 3 grams of sample (< 2 mm) were mixed with 100 ml of 1
158 M HCl solution at 200 rpm. After 2 h, the leachates were collected by filtration of the suspension
159 through 0.45 µm Millex® membrane filters.

160 2.3 Chemical analyses

161 Dissolved concentrations of iron (Fe), manganese (Mn), silicon (Si) and aluminum (Al) were analyzed
162 using an inductively coupled plasma atomic emission spectrometer (ICP-AES, ICPE-9000, Shimadzu
163 Corporation, Japan) while major coexisting cations (Ca^{2+} , Mg^{2+} , Na^+ and K^+) and anions (Cl^- , NO_3^-
164 and SO_4^{2-}) were quantified by ion chromatography (ICS-90 and ICS-1000, Dionex Corporation,
165 USA). Dissolved As concentrations greater than 0.1 mg/l were analyzed directly by ICP-AES while
166 leachates with less than 0.1 mg/l of As were first pretreated and then analyzed using an ICP-AES
167 connected to a hydride-vapor generation unit (detection limit: 0.1 µg/l). For the pretreatment of

168 leachates with As concentrations less than 0.1 mg/l, 10 ml of the leachate sample was mixed with 5 ml
169 of 12 M HCl, 0.67 ml of 20% potassium iodide (KI) solution, 0.67 ml of DI water, and 0.33 ml of 10%
170 ascorbic acid solution, and this mixture was allowed to equilibrate for 3 h prior to the chemical
171 analyses (Tabelin et al., 2013). Dissolved organic carbon (DOC) was measured by a total carbon
172 analyzer (TOC-V_{CSH}, Shimadzu Corporation, Japan) while HCO₃⁻ concentrations were estimated from
173 the alkalinity and pH using PHREEQC (Parkhurst and Appelo, 1999). The alkalinity was measured by
174 titration of a known volume of leachate with 0.02 N sulfuric acid (H₂SO₄) solution until pH 4.8 (Eang
175 et al., 2018a, b). The margins of error of the standard ICP-AES and ion chromatography were around
176 2% while the more sensitive hydride-vapor generation method for very low As concentrations had an
177 uncertainty of about 5%.

178 2.4 Geochemical modeling and multivariate statistical analysis

179 PHREEQC was used to calculate saturation indices of some important minerals in the leaching
180 experiments while the speciation diagram of As was created by the Geochemist's Workbench®
181 (Bethke and Yeakel, 2011) using actual solute activities. For data interpretation, principal component
182 analysis (PCA) was employed using Origin Pro® (OriginLab Corporation, USA). PCA is a
183 multivariate statistical method especially useful in finding correlations in very complex systems where
184 several components must be considered at the same time (i.e., high-dimensional data). This method
185 simplifies the complexity of high-dimensional data while retaining trends and patterns by transforming
186 the data into fewer “dimensions” or “summaries of features” that are called principal components (PC)
187 (Abdi and Williams, 2010). In this study, PCA was applied to sediment samples (11 parameters of 34
188 samples) and leachates obtained from the leaching experiments in DI water (16 parameters of 34
189 samples) to give additional insights into the solid-phase phase partitioning of As and the factors and
190 processes important in the release of this element into solution.

191 **3. RESULTS AND DISCUSSION**

192 3.1 Distinct lithological features of the sediments and their chemical and mineralogical compositions

193 Among the six borehole cores, those drilled in An Giang province located between the two rivers (LS
194 and PT) had layers containing exceptionally high As (Fig. 2; Supplementary Figs. 1 and 2). The
195 vertical lithofacies of these two borehole cores are composed of alternating layers of clayey silt and
196 fine sand (Fig. 2; Supplementary Table 1) and were mainly composed of SiO_2 , Al_2O_3 and Fe_2O_3 with
197 minor amounts of MgO , CaO and K_2O . The XRD patterns and their semi-quantitative analysis of
198 mineral abundances showed that quartz (SiO_2) (39–83%) is the dominant mineral in the sediment
199 samples from LS and PT with moderate to minor amounts of anorthite ($\text{CaAl}_2\text{Si}_2\text{O}_8$) (2–20%) as well
200 as moderate to trace amounts of muscovite ($(\text{K}, \text{Al})_2(\text{AlSi}_3\text{O}_{10})(\text{FOH})_2$) (up to 23%), clinocllore ($(\text{Mg},$
201 $\text{Fe})_5\text{Al}(\text{Si}_3\text{Al})\text{O}_{10}(\text{OH})_8$) (up to 16%) and kaolinite ($\text{Al}_2\text{Si}_2\text{O}_5(\text{OH})_4$) (up to 15%) (Fig. 3). Some of the
202 sediments in LS and PT also contain gypsum ($\text{CaSO}_4 \cdot 2\text{H}_2\text{O}$) and trace amounts of calcite, dolomite,
203 pyrite, goethite and hematite (Supplementary Tables 3). Moreover, two peat layers about 1-m thick
204 between depths of 15 and 25 m were observed in PT and were not present in the other five borehole
205 cores. These peat layers had lower quartz (44–46%), higher kaolinite (14–16%), more abundant TOC
206 (about 10%) and exceptionally high As contents (~33 mg/kg).

207 In contrast, the As content of sediments in borehole cores collected upstream of the Hau River
208 (Ph and P-Hu) and downstream of the Tien River (TL and TT) were all less than 20 mg/kg (Fig. 1;
209 Supplementary Figs. 1 and 2). The geological units upstream observed in Ph and P-Hu were also very
210 similar to that discussed earlier for LS and PT; that is, the vertical lithofacies are composed of
211 alternating strata of clayey silt and fine sand (Fig. 2; Supplementary Fig. 1). In comparison, TL and
212 TT had simpler vertical lithofacies than those collected upstream and were composed of coarser
213 sediments (i.e., fine to coarse sand) (Supplementary Fig. 2). In TT, for example, fine to coarse sands
214 were distributed from a depth of 5 to 40 m. It is interesting to note that in all borehole cores, SiO_2 and
215 quartz increased as the particles became coarser while as the sediments became finer, the relative
216 abundances of kaolinite, muscovite and clinocllore increased (Supplementary Tables 2–4).

217 PCA was used to extract important and inter-correlated dependent variables from the chemical
218 properties of the sediments using 11 variables (SiO_2 , Al_2O_3 , Fe_2O_3 , MgO , CaO , Na_2O , K_2O , S, As,
219 TOC and LOI) from 34 samples (Supplementary Table 5). The results showed that three PCs had
220 eigenvalues > 1, and they accounted for 82.9% of the total “inertia” of the composition of sediments.

221 PC 1 (49.07%) had high loadings of Al₂O₃, Fe₂O₃, MgO, K₂O, As and TOC, which relates the As
222 content of sediments to clay and phyllosilicate minerals, Fe-bearing minerals, organic matter and
223 carbonates. This means that most of As are closely associated with these minerals and phases found in
224 the sediments, a generalization that will be discussed in more detail in the next subsection. Meanwhile,
225 PC 2 (24.37%) and PC 3 (9.47%) could be related to the depositional processes that occurred during
226 the delta's formation that include submersion in seawater and dolomite deposition under organic-rich
227 environments (Supplementary information).

228 3.2 Solid-phase partitioning of As and its mobility under oxic, acidic and reducing conditions

229 The solid-phase partitioning of As in sediments from the six borehole cores and the leaching behavior
230 of As with depth under oxic, acidic and reducing are illustrated in Fig. 4 and Supplementary Figs. 3
231 and 4. Leachability, L_i (mg/kg or $\mu\text{g}/\text{kg}$), was used instead of concentration to normalize the results
232 because the weight of samples and volume of leachants used in the three types of leaching experiments
233 were slightly different (Tamoto et al., 2015; Tabelin et al., 2017a). It was calculated as

$$234 \quad L_i = \frac{C_{As} * V_L}{M_s} \quad (1)$$

235 where C_{As} is the concentration of As in the leachate, V_L is the volume of leachant, and M_s is the mass
236 of sample used in the leaching experiments.

237 Sediments collected between the Tien and Hau Rivers (LS and PT) had substantially higher
238 amounts of As partitioned with the organic/sulfides fraction compared with the other borehole core
239 samples (Figs. 1 and 4; Supplementary Figs. 3 and 4). In LS, for example, As associated with the
240 organic/sulfide phase accounted for 25–41% of the total As content of the sediments. Arsenic found
241 with the exchangeable fraction was also substantial (13–30%) while those associated with Fe-Mn
242 oxides and carbonates were quite low at 3–7% and 1–3%, respectively. Among the sediment samples,
243 those from the peat layers in PT had the highest As associated with the exchangeable (~9 mg/kg) and
244 organic/sulfide (10–12 mg/kg) phases, the sum of which was even higher than the total As content of
245 the other samples. There are three possible explanations for this exceptionally high As in the
246 exchangeable and organic/sulfide fractions of sediments from the peat layers. First, organic particles in
247 these layers contained substantial amounts of As-bearing framboidal and euhedral pyrite (Figs. 5 and

248 6). Framboidal pyrite is typically formed in the anoxic-oxic sediment interface of estuarine systems,
249 ancient marshlands and shallow seas when both the supply of organic carbon and the rate of sulfate
250 reduction are low while single euhedral pyrite crystals are formed when organic matter is rich and
251 sulfate reduction is rapid (Berner, 1984; Goldhaber and Kalan, 1974; Howarth and Teal, 1979;
252 Rickard, 1975; Tabelin et al., 2012a). Second, As is known to strongly adsorb to organic matter like
253 peat, lignite and coal (Besold et al., 2018; Mar et al., 2013; Wang and Mulligan 2006). Third, soluble
254 salt-like phases, kaolinite, muscovite and clinocllore, which are known to incorporate or adsorb As
255 (Beaulieu and Savage, 2005; Charlet et al., 2007; Goldberg and Glaubig, 1988; Tabelin et al., 2014b,
256 2017b), were abundant in the peat layers (Supplementary Fig. 5; Supplementary Table 3).

257 In contrast, As in sediment samples from the other four borehole cores (Ph, P-Hu, TL and TT)
258 were partitioned mostly with the exchangeable fraction (20–49%). Arsenic in this fraction is likely
259 associated with soluble salts (Supplementary Fig. 5) and weakly or strongly sorbed to
260 clays/phyllsilicates and Fe-oxyhydroxides/oxides (Fig. 3; Supplementary Fig. 6). The partitioning of
261 As in salt-like phases have also been noted in sedimentary rocks (Tabelin et al., 2012b; 2017a) while
262 the sorption of As to clays/phyllsilicates and Fe-oxyhydroxides/oxides is well documented in the
263 literature (Beaulieu and Savage, 2005; Fendorf et al., 1997; Garcia-Ordiales et al., 2018; Manning and
264 Goldberg, 1996; Tabelin et al., 2013, 2014c; Waychunas et al., 1993, 2005; Yang et al., 2016). Other
265 important As-hosting phases in the sediments of these four borehole cores include the Fe-Mn oxides
266 (2–13%) (Supplementary Figs. 6 and 7), which are readily dissolved under reducing conditions
267 (Stumm and Sulzberger, 1992), and the organic/sulfide fraction (2–15%) that dissociate under oxic
268 conditions (Tabelin et al., 2017c, d).

269 The leachates from the sediments under oxic conditions could be divided into four groups: (i)
270 acidic (pH < 4.5), (ii) circumneutral (pH around 6–8), (iii) weakly alkaline (pH around 8–9), and (iv)
271 moderately alkaline (pH > 9). Acidic leachates were measured in the upper clayey silt layers (above 5
272 m) of LS and PT, in one of the peat layers of PT, and in the medium sand layer of TT at a depth of
273 around 25 m (Fig. 7; Supplementary Figs. 8 and 9). Based on the characterization and leaching results,
274 there are two possible sources of acidity in the sediments: (1) acid sulfate soils (Fig. 7; Nguyen and
275 Itoi, 2009), (2) pyrite oxidation (Figs. 5 and 6; Park et al., 2019; Tabelin and Igarashi, 2009; Tatsuhara

276 et al., 2012; Tomiyama et al., 2019), and (3) decomposition of organic matter (Wang and Mulligan,
277 2006). Meanwhile, the slightly alkaline leachates measured in the upper clayey silt layer of Ph and P-
278 Hu could be attributed to their considerable calcite and dolomite contents, which are known to control
279 the pH of soil, rock and sediment systems due to their higher solubility compared with sulfide and
280 silicate minerals (Plummer et al., 1978; Tabelin et al., 2012c, d). For the exceptionally high pH from
281 the brownish silty clay layer of TT, one possible reason is the presence of nahcolite (NaHCO_3), a
282 soluble salt sometimes found in sediments and sedimentary rocks (Sugitani et al., 2003; Tabelin et al.,
283 2017a). This deduction is consistent with the higher Na^+ (about 50 mg/l) and HCO_3^- (about 132 mg/l)
284 concentrations in the leachate of this sediment compared with the rest of the samples.

285 Dissolved As in leachates of the oxic leaching experiments (DI water) was likely dominated by
286 arsenate (As^{V}) based on the Eh-pH diagram shown in Supplementary Fig. 11. Among the sediment
287 samples, those collected from the peat layers in PT and the brownish silty clay layer in TT had the
288 highest As leachabilities in DI water at > 0.4 mg/kg (> 44 $\mu\text{g/L}$) (Fig. 7; Supplementary Fig. 9). As
289 discussed previously, the peat layers were rich in As-containing pyrite, organic matter, kaolinite,
290 muscovite and clinocllore while the bulk of As in the peat layers are associated with exchangeable
291 and organic/sulfide phases, so under acidic conditions, the release of As was likely controlled by
292 pyrite oxidation/organic matter dissociation, proton-promoted dissolution, and adsorption-desorption
293 reactions. Pyrite and organic matter are readily oxidized in the presence of oxygen, a process that
294 releases their As load into solution (Kim et al., 2002; Kinsela et al., 2011; Tabelin and Igarashi 2009;
295 Wang and Mulligan, 2006). In addition, functional groups of dissolved organic matter (DOM) like
296 catechol are known to coordinate with metal ions like Ti^{4+} , Al^{3+} and Fe^{3+} via complexation reactions,
297 increasing their solubility and affecting the electrochemical properties of pyrite and arsenopyrite (Li et
298 al., 2019a, b; Park et al., 2018a). Although clays and phyllosilicates are better As adsorbents between
299 pH 4 and 6, their sorption ability was likely depressed by the relatively high concentrations of
300 dissolved Si and DOC, both of which are known to compete with As for sorption sites (Fig. 7; Han et
301 al., 2013; Tabelin et al., 2018; Wang and Mulligan, 2006; Xue et al., 2019). In comparison, the
302 brownish clayey silt layer found in TT contained only about half of As found in the peat layers (~ 17
303 mg/kg) but released similarly high amounts of As into solution (~ 46 $\mu\text{g/l}$), which could be attributed to

304 the strongly alkaline pH of the leachate (about 9.5) that enhanced not only desorption reactions of
305 exchangeable phases but also the oxidation of As-bearing pyrite (Beaulieu and Savage, 2005; Manning
306 and Goldberg, 1996; Tabelin and Igarashi, 2009; Tabelin et al., 2018).

307 To identify the factors responsible for the observed leachate chemistry when the sediments are
308 in contact with DI water, PCA was applied to 16 parameters (pH, EC, Eh, Na⁺, K⁺, Mg²⁺, Ca²⁺, Fe, Al,
309 dissolved Si, As, Cl⁻, NO₃⁻, SO₄²⁻, HCO₃⁻ and DOC) of the 34 leachate samples. Three PCs had
310 eigenvalues > 1 and they accounted for 85.8% of the total “inertia” of measured leachate chemistries
311 (Supplementary Table 6). PC 1 (46.36%) showed high loadings of Na⁺, K⁺, Mg²⁺, Fe, Al, dissolved Si,
312 As and NO₃⁻, which could infer that this principal component is related to the strong effects of clay
313 and phyllosilicate minerals (i.e., kaolinite, muscovite and clinochlore) on the leachate chemistry
314 including the release of As, which are consistent with our earlier deductions. PC 2 (19.4%) had high
315 positive loadings of EC, Eh, Mg²⁺, Ca²⁺ and SO₄²⁻ together with high negative loadings of pH.
316 Because SO₄²⁻, Na⁺ and EC had the highest contributions to PC 2, this component could be related to
317 the major coexisting ions controlling the EC of the leachates (Fig. 7; Supplementary Figs. 8 and 9).
318 Meanwhile, the positive loading of Eh and negative loading of pH could be explained by the enhanced
319 oxidation of pyrite, which makes the pH more acidic, at higher Eh values (Tabelin et al., 2018).
320 Finally, PC 3 (14.98%) had high positive loadings of pH and HCO₃⁻ as well as high negative loadings
321 of DOC and Cl⁻. The high positive loadings of HCO₃⁻ and pH could be related to the pH control
322 exerted by carbonate-bearing minerals, which is consistent with our earlier deduction, while the
323 negative loadings of DOC and Cl⁻ could be explained by the substantial pyrite content of the organic-
324 rich parts of the sediments and its enhanced oxidation in the presence of Cl⁻, both of which lowers the
325 HCO₃⁻ concentration and pH of leachates.

326 Acidification and reducing conditions both enhanced the release of As from all sediment
327 samples in the six borehole cores (Fig. 4; Supplementary Figs. 3 and 4). For example, the leachability
328 of As under reducing conditions increased by at least 30- and 50-fold in Ph and P-Hu, respectively,
329 compared with that in DI water. The release of As in the sediments was even more dramatic under
330 acidic conditions whereby As concentrations increased by at least 50 and 100 times in Ph and P-Hu,
331 respectively compared with those measured in DI water (Supplementary Fig. 3). The higher

332 leachability of As in HCl (acidic condition) than $\text{Na}_2\text{S}_2\text{O}_4$ (reducing condition) could be attributed to
333 two processes: (1) reducing conditions and high dissolved S concentration may induce the re-
334 precipitation of Fe-sulfides that immobilizes a portion of dissolved As (Van Geen et al., 2004; Zheng
335 et al., 2004), and (2) Cl^- could enhance pyrite oxidation and As release into solution via aggressively
336 replacing surface bound hydroxyl ions to form more soluble iron-chloride complexes and suppressing
337 the formation of a passivating sulfur-rich layer on pyrite (Lehmann et al., 2000; Park et al., 2018b).

338 3.3 Implications to the geochemistry of arsenic in aquifer sediments

339 The results of this study provide compelling evidence that the roles played by clay minerals and
340 phyllosilicates in the release and migration of As in naturally contaminated aquifer systems are as
341 important as those of pyrite and iron-oxyhydroxides/oxides. Although clay and phyllosilicate minerals
342 have been recognized as important players in the mobility of As in the Ganges Delta (Acharyya et al.,
343 2000; Charlet et al., 2007), very few studies have reported that they also play important roles in As
344 geochemistry of groundwater in the Mekong Delta. Depending on prevailing geochemical conditions,
345 these minerals could act as either sinks or sources of dissolved As. For example, slightly acidic pH and
346 oxidizing conditions promote the immobilization of As via sorption reactions while under slightly
347 alkaline conditions, they become sources of As and releases this element via desorption. Sorption-
348 desorption reactions of As with these minerals are also strongly affected by the concentrations of
349 coexisting ions that compete with As for adsorption sites like dissolved Si and DOC. Our results also
350 suggest that the high SO_4^{2-} concentration of leachates from the organic-rich layers (e.g., peat layers in
351 PT) was largely due to the dissolution of soluble salt-like phases like gypsum (e.g., the saturation
352 index (*SI*) of gypsum from PT-6 was around -0.48) rather than the oxidation of pyrite. Finally, the
353 reductive dissolution of As-bearing iron-oxyhydroxides was not the only process by which As could
354 be released from sediments of the Mekong Delta. Drying-flooding/inundation cycles that promote
355 acidification of the upper layers of the aquifer as well as Cl^- -enhanced pyrite oxidation from salt-water
356 intrusion due to the excessive abstraction of groundwater for municipal, industrial or agricultural uses
357 could exacerbate the problem of As-contaminated groundwater in the future.

358 4. CONCLUSIONS

359 This study investigated the solid-phase partitioning of As in sediments of borehole cores collected
360 from the Vietnamese-side of the Mekong Delta and how As is released under oxic, acidic and reducing
361 conditions. The findings of this study are summarized as follows:

- 362 1. Substantial amounts of As were bound with the exchangeable phases, which were strongly
363 influenced by small variations in pH and the presence of coexisting ions competing with As for
364 adsorption sites like dissolved Si and DOC.
- 365 2. Kaolinite, muscovite and clinocllore were important sources/sinks of dissolved As depending on
366 the pH and concentrations of coexisting ions.
- 367 3. Peat layers were found in the sediments that contained substantial amounts of As-rich framboidal
368 and euhedral pyrite.
- 369 4. The release of As from the sediments was enhanced under acidic conditions via the dissociation
370 of Fe-oxyhydroxides/oxides, clay minerals and phyllosilicates as well as the enhanced oxidation
371 of pyrite due to Cl^- .
- 372 5. Arsenic mobility in the sediments was enhanced under reducing conditions via the reductive
373 dissolution of iron-oxyhydroxides/oxides.
- 374 6. The shallow aquifer of the Mekong Delta is prone to dramatic geochemical variations due to
375 human-induced activities and the climate/topography of the region that may enhance the release
376 of As from sediments into the groundwater.

377 **Acknowledgments**

378 This study was financially supported by the Japan International Cooperation Agency (JICA) through
379 the AUN-Seed Net Collaborative Research Program for Common Regional Issues (CRC) in ASEAN-
380 2016. The authors also wish to thank Dr. Xinde Cao and the anonymous reviewers for their valuable
381 inputs to this paper.

382

383 **Figure Captions**

384

385 FIG. 1 A map of Vietnam superimposed with the location of borehole cores used in
386 this study.

387

388 FIG. 2 Chemical compositions of distinct lithological features in borehole cores
389 obtained between the Hau and Tien Revers (LS and PT): (a-1) variation of
390 major chemical components in LS with depth, (a-2) distribution of trace
391 components (As, S, and TOC) in LS with depth, (b-1) variation of major
392 chemical components in PT with depth, and (b-2) distribution of trace
393 components (As, S, and TOC) in PT with depth.

394

395 FIG. 3 SEM photomicrographs and semi-quantitative point analyses of (a)
396 clinocllore, (b) muscovite, and (c) kaolinite.

397

398 FIG. 4 Solid-phase partitioning and leaching behaviors of As with depth under
399 various conditions: (a-1) As distribution in exchangeable, carbonate, Fe-Mn
400 oxides (reducible), organic and sulfides, and residual phases of LS
401 sediments, (a-2) As leachability with depth under oxidizing (DI water)
402 conditions in LS, (a-3) As leachability with depth under acidic (HCl) and
403 reducing ($S_2O_4^{2-}$) conditions in LS, (b-1) As distribution in exchangeable,
404 carbonate, Fe-Mn oxides (reducible), organic and sulfides, and residual
405 phases of PT sediments, (b-2) As leachability with depth under oxidizing (DI
406 water) conditions in PT, (b-3) As leachability with depth under acidic (HCl)
407 and reducing ($S_2O_4^{2-}$) conditions in PT.

408 FIG. 5 SEM photomicrographs of pyrite-rich organic particles in the peat layers of
409 PT containing (a-1) framboidal pyrite with the (a-2) EDS spectra of selected
410 areas (a-2) and (b-1) subhedral pyrite with the (b-2) EDS spectra of selected
411 areas.

412 FIG. 6 SEM photomicrographs of As-bearing framboidal pyrite (a-1) and the
413 corresponding elemental maps of As (a-2), Fe (a-3), S (a-4), O (a-5), and Si
414 (a-6), and SEM photomicrographs of As-bearing framboidal/euhedral pyrite
415 and Al/Fe oxyhydroxides (b-1) and the corresponding elemental maps of As
416 (a-2), Fe (a-3), S (a-4), Al (a-5), and O (a-6).

417 FIG. 7 Vertical distribution of pH and coexisting ions from the leaching
418 experiments using DI water: (a-1) pH with depth in LS, (a-2) Na^+ , K^+ , Fe and
419 Al concentrations with depth in LS, (a-3) dissolved Si, SO_4^{2-} , DOC
420 concentrations with depth in LS, (b-1) pH with depth in PT, (b-2) Na^+ , K^+ ,
421 Fe and Al concentrations with depth in PT, (b-3) dissolved Si, SO_4^{2-} , DOC
422 concentrations with depth in PT.

423 **References**

- 424 Abdi, H., Williams, L.J., 2010. Principal component analysis. Wiley interdisciplinary reviews:
425 Computational statistics 2, 433–459.
- 426 Acharyya, S.K., Lahiri, S., Raymahashay, B.C., Bhowmik, A., 2000. Arsenic toxicity of groundwater
427 in parts of the Bengal basin in India and Bangladesh: The role of Quaternary stratigraphy and
428 Holocene sea-level fluctuation. *Environ. Geol.* 39, 1127–1137.
- 429 Beaulieu, B.T., Savage, K.S., 2005. Arsenate adsorption structures on aluminum oxide and
430 phyllosilicate mineral surfaces in smelter-impacted soils. *Environ. Sci. Technol.* 39, 3571–3579.
- 431 Berg, M., Stengel, C., Trang, P.T.K., Viet, P.H., Sampson, M.L., Leng, M., Samreth, S., Fredericks,
432 D., 2007. Magnitude of arsenic pollution in the Mekong and Red River Deltas—Cambodia and
433 Vietnam. *Sci. Total Environ.* 372, 413–425.
- 434 Berner, R.A., 1984. Sedimentary pyrite formation: An update. *Geochim. Cosmochim. Acta* 48, 605-
435 615.
- 436 Besold, J., Biswas, A., Suess, E., Scheinost, A.C., Rossberg, A., Mikutta, C., Kretzschmar, R.,
437 Gustafsson, J.P., Planer-Friedrich, B., 2018. Monothioarsenate transformation kinetics determines
438 arsenic sequestration by sulfhydryl groups of peat. *Environ. Sci. Technol.* 52, 7317–7326.
- 439 Bethke, C.M., Yeakel, S., 2011. The Geochemist's Workbench® – a User's Guide to GSS, Rxn, Act2,
440 Tact, Spec8, React, Gtplot, X1t, X2t and Xtplot. Aqueous Solutions LLC, Urbana, Illinois.
- 441 Charlet, L., Chakraborty, S., Appelo, C.A.J., Roman-Ross, G., Nath, B., Ansari, A.A., Lanson, M.,
442 Chatterjee, D., Mallik, S.B., 2007. Chemodynamics of an arsenic “hotspot” in a West Bengal
443 aquifer: A field and reactive transport modeling study. *Appl. Geochem.* 22, 1273–1292.
- 444 Clevenger, T.E., 1990. Use of sequential extraction to evaluate the heavy metals in mining wastes.
445 *Water Air Soil Poll.* 50, 241–253.
- 446 Eang, K.E., Igarashi, T., Fujinaga, R., Kondo, M. and Tabelin, C.B., 2018a. Groundwater monitoring
447 of an open-pit limestone quarry: groundwater characteristics, evolution and their connections to
448 rock slopes. *Environmen. Monit. Assess.* 190(4), 193.
- 449 Eang, K.E., Igarashi, T., Kondo, M., Nakatani, T., Tabelin, C.B., Fujinaga, R., 2018b. Groundwater
450 monitoring of an open-pit limestone quarry: Water-rock interaction and mixing estimation within
451 the rock layers by geochemical and statistical analyses. *Int. J. Min. Sci. Technol.* 28, 849–857.

452 Feldman, P.R., Rosenboom, J.W., 2001. Cambodia drinking water quality assessment. Phnom Penh,
453 Cambodia: World Health Organisation of the UN [WHO] in cooperation with Cambodian
454 Ministry of Rural Development and the Ministry of Industry, Mines and Energy.

455 Fendorf, S., Eick, M.J., Grossl, P., Sparks, D.L., 1997. Arsenate and chromate retention mechanisms
456 on goethite. 1. Surface structure. *Environ. Sci. Technol.* 31, 315–320.

457 Fendorf, S., Michael, H.A., Van Geen, A., 2010. Spatial and temporal variations of groundwater
458 arsenic in South and Southeast Asia. *Science*, 328, 1123–1127.

459 Garcia-Ordiales, E., Covelli, S., Rico, J.M., Roqueñí, N., Fontolan, G., Flor-Blanco, G., Cienfuegos,
460 P., Loredó, J., 2018. Occurrence and speciation of arsenic and mercury in estuarine sediments
461 affected by mining activities (Asturias, northern Spain). *Chemosphere* 198, 281–289.

462 Goldberg, S., Glaubig, R.A., 1988. Anion sorption on a calcareous, montmorillonitic soil–arsenic. *Soil*
463 *Sci. Soc. Am. J.* 52, 1297–1300.

464 Goldhaber, M.B., Kalan, I.R., The sulfur cycle, in: E.D. Goldberg (Ed.), *The Sea, Marine Chemistry*
465 *Vol. 5*, Wiley-Interscience, New York, 1974, pp. 527-655.¥

466 Han, Y.S., Demond, A.H., Hayes, K.F., 2013. Impact of dissolved silica on arsenite removal by nano-
467 particulate FeS and FeS-coated sand. *Chemosphere* 92, 477–481.

468 Harvey, C.F., Swartz, C.H., Badruzzaman, A.B.M., Keon-Blute, N., Yu, W., Ali, M.A., Jay, J.,
469 Beckie, R., Niedan, V., Brabander, D., Oates, P.M., 2002. Arsenic mobility and groundwater
470 extraction in Bangladesh. *Science* 298, 1602–1606.

471 Hoang, T.H., Bang, S., Kim, K.W., Nguyen, M.H., Dang, D.M., 2010. Arsenic in groundwater and
472 sediment in the Mekong River delta, Vietnam. *Environ. Pollut.* 158, 2648–2658.

473 Howarth, R.W., Teal, J.M., 1979. Sulfate reduction in a New England salt marsh. *Limnol.*
474 *Oceanogr.* 24, 999–1013.

475 Kim, M.J., Ahn, K.H., Jung, Y., 2002. Distribution of inorganic arsenic species in mine tailings of
476 abandoned mines from Korea. *Chemosphere* 49, 307–312.

477 Kinsela, A.S., Collins, R.N., Waite, T.D., 2011. Speciation and transport of arsenic in an acid sulfate
478 soil-dominated catchment, eastern Australia. *Chemosphere* 82, 879–887.

479 Kocar, B.D., Polizzotto, M.L., Benner, S.G., Ying, S.C., Ung, M., Ouch, K., Samreth, S., Suy, B.,
480 Phan, K., Sampson, M., Fendorf, S., 2008. Integrated biogeochemical and hydrologic processes

481 driving arsenic release from shallow sediments to groundwaters of the Mekong delta. Appl.
482 Geochem. 23, 3059–3071.

483 Li, X., Hiroyoshi, N., Tabelin, C.B., Naruwa, K., Harada, C., Ito, M., 2019a. Suppressive effects of
484 ferric-catecholate complexes on pyrite oxidation. Chemosphere 214, 70-78.

485 Li, X., Gao, M., Hiroyoshi, N., Tabelin, C.B., Taketsugu, T., Ito, M., 2019b. Suppression of pyrite
486 oxidation by ferric-catecholate complexes: An electrochemical study. Miner. Eng. 138, 226–237.

487 Manning, B.A., Goldberg, S., 1996. Modeling arsenate competitive adsorption on kaolinite,
488 montmorillonite and illite. Clay Clay Miner. 44, 609–623.

489 Mar, K.K., Karnawati, D., Putra, D.P.E., Igarashi, T., Tabelin, C.B., 2013. Comparison of arsenic
490 adsorption on lignite, bentonite, shale, and iron oxide from Indonesia. Procedia Earth Planet. Sci.
491 6, 242–250.

492 Marumo, K., Ebashi, T., Ujiie, T., 2003. Heavy metal concentrations, leachabilities and lead isotope
493 ratios of Japanese soils. Shigen-Chishitsu 53, 125–146. [Paper in Japanese with English abstract].

494 Nguyen, K.P., Itoi, R., 2009. Source and release mechanism of arsenic in aquifers of the Mekong
495 Delta, Vietnam. J. Contam. Hydrol. 103, 58–69.

496 Nguyen, V.L., Ta, T.K.O., Tateishi, M., 2000. Late Holocene depositional environments and coastal
497 evolution of the Mekong River Delta, Southern Vietnam. J. Asian Earth Sci. 18, 427–439.

498 Park, I., Tabelin, C.B., Magaribuchi, K., Seno, K., Ito, M., Hiroyoshi, N., 2018a. Suppression of the
499 release of arsenic from arsenopyrite by Carrier-microencapsulation using Ti-catechol complex. J.
500 Hazard Mater. 344, 322-332.

501 Park, I., Tabelin, C.B., Seno, K., Jeon, S., Ito, M., Hiroyoshi, N., 2018b. Simultaneous suppression of
502 acid mine drainage formation and arsenic release by carrier-microencapsulation using aluminum-
503 catecholate complexes. Chemosphere 205, 414–425.

504 Park, I., Tabelin, C.B., Jeon, S., Li, X., Seno, K., Ito, M. and Hiroyoshi, N., 2019. A review of recent
505 strategies for acid mine drainage prevention and mine tailings recycling. Chemosphere 219, 588–
506 606.

507 Parkhurst, D.L., Appelo, C.A.J., 1999. User's guide to PHREEQC (version 2) – a computer program
508 for speciation, batch-reactions, one-dimensional transport, and inverse geochemical calculations.
509 U.S. Department of the Interior and U.S. Geological Survey. Water Resour. Invest. Rep. 99–
510 4259.

511 Pham, V.N., Boyer, D., Le Mouél, J.L., Nguyen, T.K.T., 2002. Hydrogeological investigation in the
512 Mekong Delta around Ho-Chi-Minh City (South Vietnam) by electric tomography. *C. R.*
513 *Geosci.* 334, 733–740.

514 Polizzotto, M.L., Kocar, B.D., Benner, S.G., Sampson, M., Fendorf, S., 2008. Near-surface wetland
515 sediments as a source of arsenic release to ground water in Asia. *Nature* 454, 505.

516 Rickard, D.T., 1975. Kinetics and mechanism of pyrite formation at low temperatures. *Am. J.*
517 *Sci.* 275, 636–652.

518 Silveira, M.L., Alleoni, L.R.F., O'Connor, G.A., Chang, A.C., 2006. Heavy metal sequential
519 extraction methods – a modification for tropical soils. *Chemosphere* 64, 1929–1938.

520 Smedley, P.L., Kinniburgh, D.G., 2002. A review of the source, behavior, and distribution of arsenic
521 in natural waters. *Appl. Geochem.* 17, 517–568.

522 Stumm, W., Sulzberger, B., 1992. The cycling of iron in natural environments: Considerations based
523 on laboratory studies of heterogeneous redox processes. *Geochim. Cosmochim. Acta* 56, 3233–
524 3257.

525 Tabelin, C.B., Igarashi, T., 2009. Mechanisms of arsenic and lead release from hydrothermally altered
526 rock. *J. Hazard. Mater.* 169, 980–990.

527 Tabelin, C.B., Igarashi, T., Tamoto, S., Takahashi, R., 2012a. The roles of pyrite and calcite in the
528 mobilization of arsenic and lead from hydrothermally altered rocks excavated in Hokkaido,
529 Japan. *J. Geochem. Explor.* 119–120, 17–31.

530 Tabelin, C.B., Basri, A.H.M., Igarashi, T., Yoneda, T., 2012b. Removal of arsenic, boron, and
531 selenium from excavated rocks by consecutive washing. *Water Air Soil Poll.* 223, 4153–4167.

532 Tabelin, C.B., Igarashi, T., Takahashi, R., 2012c. Mobilization and speciation of arsenic from
533 hydrothermally altered rock in laboratory column experiments under ambient conditions. *Appl.*
534 *Geochem.* 27, 326–342.

535 Tabelin, C.B., Igarashi, T., Yoneda, T., 2012d. Mobilization and speciation of arsenic from
536 hydrothermally altered rock containing calcite and pyrite under anoxic conditions. *Appl.*
537 *Geochem.* 27, 2300–2314.

538 Tabelin, C.B., Igarashi, T., Yoneda, T., Tamamura, S., 2013. Utilization of natural and artificial
539 adsorbents in the mitigation of arsenic leached from hydrothermally altered rock. *Eng. Geol.* 156,
540 58–67.

541 Tabelin, C.B., Hashimoto, A., Igarashi, T., Yoneda, T., 2014a. Leaching of boron, arsenic and
542 selenium from sedimentary rocks: I. Effects of contact time, mixing speed and liquid-to-solid
543 ratio. *Sci. Total Environ.* 472, 620–629.

544 Tabelin, C.B., Hashimoto, A., Igarashi, T., Yoneda, T., 2014b. Leaching of boron, arsenic, and
545 selenium from sedimentary rocks: II. pH dependence, speciation, and mechanisms of release. *Sci.*
546 *Total Environ.* 473–474, 244–253.

547 Tabelin, C.B., Igarashi, T., Arima, T., Sato, D., Tatsuhara, T., Tamoto, S., 2014c. Characterization and
548 evaluation of arsenic and boron adsorption onto natural geologic materials, and their application
549 in the disposal of excavated altered rock. *Geoderma* 213, 163–172.

550 Tabelin, C.B., Sasaki, R., Igarashi, T., Park, I., Tamoto, S., Arima, T., Ito, M., Hiroyoshi, N., 2017a.
551 Simultaneous leaching of arsenite, arsenate, selenite, and selenate, and their migration in tunnel-
552 excavated sedimentary rocks: I. Column experiments under intermittent and unsaturated flow.
553 *Chemosphere* 186, 558–569.

554 Tabelin, C.B., Sasaki, R., Igarashi, T., Park, I., Tamoto, S., Arima, T., Ito, M., Hiroyoshi, N., 2017b.
555 Simultaneous leaching of arsenite, arsenate, selenite, and selenate, and their migration in tunnel-
556 excavated sedimentary rocks: II. Kinetic and reactive transport modeling. *Chemosphere* 188,
557 444–454.

558 Tabelin, C.B., Veerawattananun, S., Ito, M., Hiroyoshi, N., Igarashi, T., 2017c. Pyrite oxidation in the
559 presence of hematite and alumina: I. Batch leaching experiments and kinetic modeling
560 calculations. *Sci. Total Environ.* 580, 687–689.

561 Tabelin, C.B., Veerawattananun, S., Ito, M., Hiroyoshi, N., Igarashi, T., 2017d. Pyrite oxidation in the
562 presence of hematite and alumina: II. Effects on the cathodic and anodic half-cell reactions. *Sci.*
563 *Total Environ.* 581–582, 126–135.

564 Tabelin, C.B., Igarashi, T., Villacorte-Tabelin, M., Park, I., Opiso, E.M., Ito, M., Hiroyoshi, N., 2018.
565 Arsenic, selenium, boron, lead, cadmium, copper, and zinc in naturally contaminated rocks: A
566 review of their sources, modes of enrichment, mechanisms of release, and mitigation
567 strategies. *Sci. Total Environ.* 645, 1522–1553.

568 Tamoto, S., Tabelin, C.B., Igarashi, T., Ito, M., Hiroyoshi, N., 2015. Short and long term release
569 mechanisms of arsenic, selenium and boron from tunnel-excavated sedimentary rock under in situ
570 conditions. *J. Contam. Hydrol.* 175–176, 60–71.

571 Tatsuhara, T., Arima, T., Igarashi, T., & Tabelin, C. B. (2012). Combined neutralization–adsorption
572 system for the disposal of hydrothermally altered excavated rock producing acidic leachate with
573 hazardous elements. *Eng. Geol.* 139, 76-84.

574 Tessier, A., Campbell, G.C., Bisson, M., 1979. Sequential extraction procedure for the speciation of
575 particulate trace metals. *Anal. Chem.* 51, 844–850.

576 Tomiyama, S., Igarashi, T., Tabelin, C.B., Tangviroon, P. and Ii, H., 2019. Acid mine drainage
577 sources and hydrogeochemistry at the Yatani mine, Yamagata, Japan: A geochemical and isotopic
578 study. *J. Contam. Hydrol.*, <https://doi.org/10.1016/j.jconhyd.2019.103502>

579 Van Geen, A., Rose, J., Thorall, S., Garnier, J.M., Zheng, Y., Bottero, J.Y., 2004. Decoupling of As
580 and Fe release to Bangladesh groundwater under reducing conditions. Part II: Evidence from
581 sediment incubations. *Geochim. Cosmochim. Acta* 68, 3475–3486.

582 Wang, S., Mulligan, C.N., 2006. Natural attenuation processes for remediation of arsenic
583 contaminated soils and groundwater. *J. Hazard. Mater.* B138, 459–470.

584 Waychunas, G.A., Rea, B.A., Davis, J.A., Fuller, C.C., 1993. Surface chemistry of ferrihydrite: I.
585 EXAFS studies of the geometry of coprecipitated and adsorbed arsenate. *Geochim. Cosmochim.*
586 *Acta* 57, 2251–2269.

587 Waychunas, G.A., Trainor, T., Eng, P., Catalano, J., Brown, G., Davis, J., Rogers, J., Bargar, J., 2005.
588 Surface complexation studied via combined grazing-incidence EXAFS and surface diffraction:
589 Arsenate on hematite (0001) and (1012). *Anal. Bioanal. Chem.* 383, 12–27.

590 Xue, Q., Ran, Y., Tan, Y., Peacock, C.L., Du, H., 2019. Arsenite and arsenate binding to ferrihydrite
591 organo-mineral coprecipitate: Implications for arsenic mobility and fate in natural
592 environments. *Chemosphere* 224, 103–110.

593 Yang, H.J., Lee, C.Y., Chiang, Y.J., Jean, J.S., Shau, Y.H., Takazawa, E., Jiang, W.T., 2016.
594 Distribution and hosts of arsenic in a sediment core from the Chianan Plain in SW Taiwan:
595 Implications on arsenic primary source and release mechanisms. *Sci. Total Environ.* 569, 212–
596 222.

597 Zheng, Y., Stute, M., Van Geen, A., Gavrieli, I., Dhar, R., Simpson, H.J., Schlosser, P., Ahmed, K.M.,
598 2004. Redox control of arsenic mobilization in Bangladesh groundwater. *Appl. Geochem.* 19,
599 201–214.

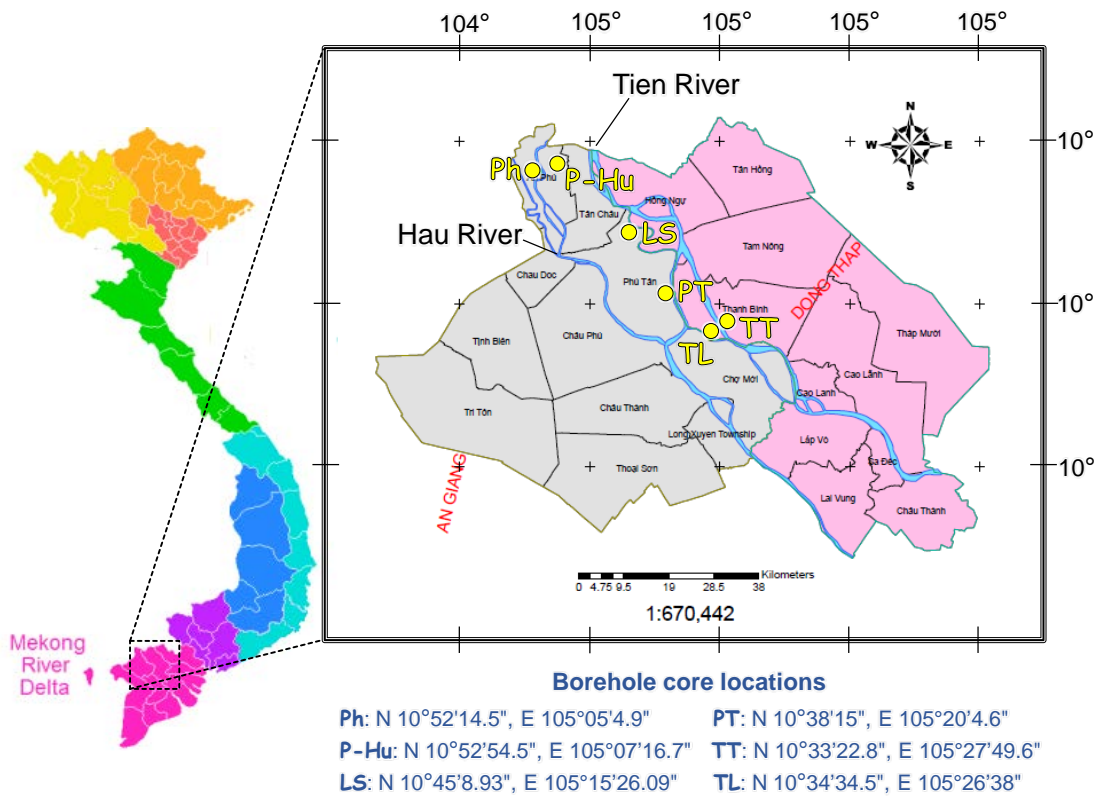


Figure 1

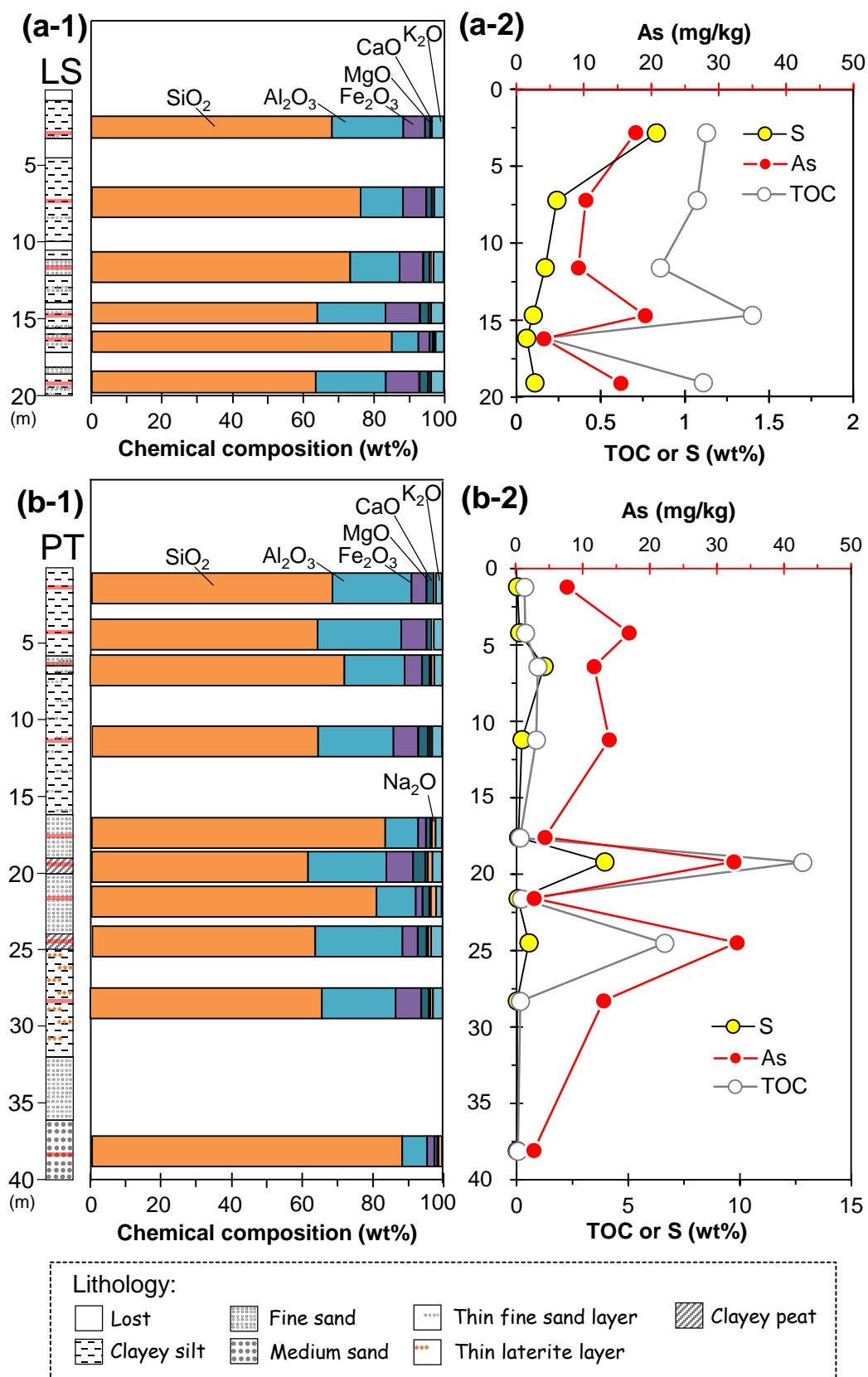


Figure 2

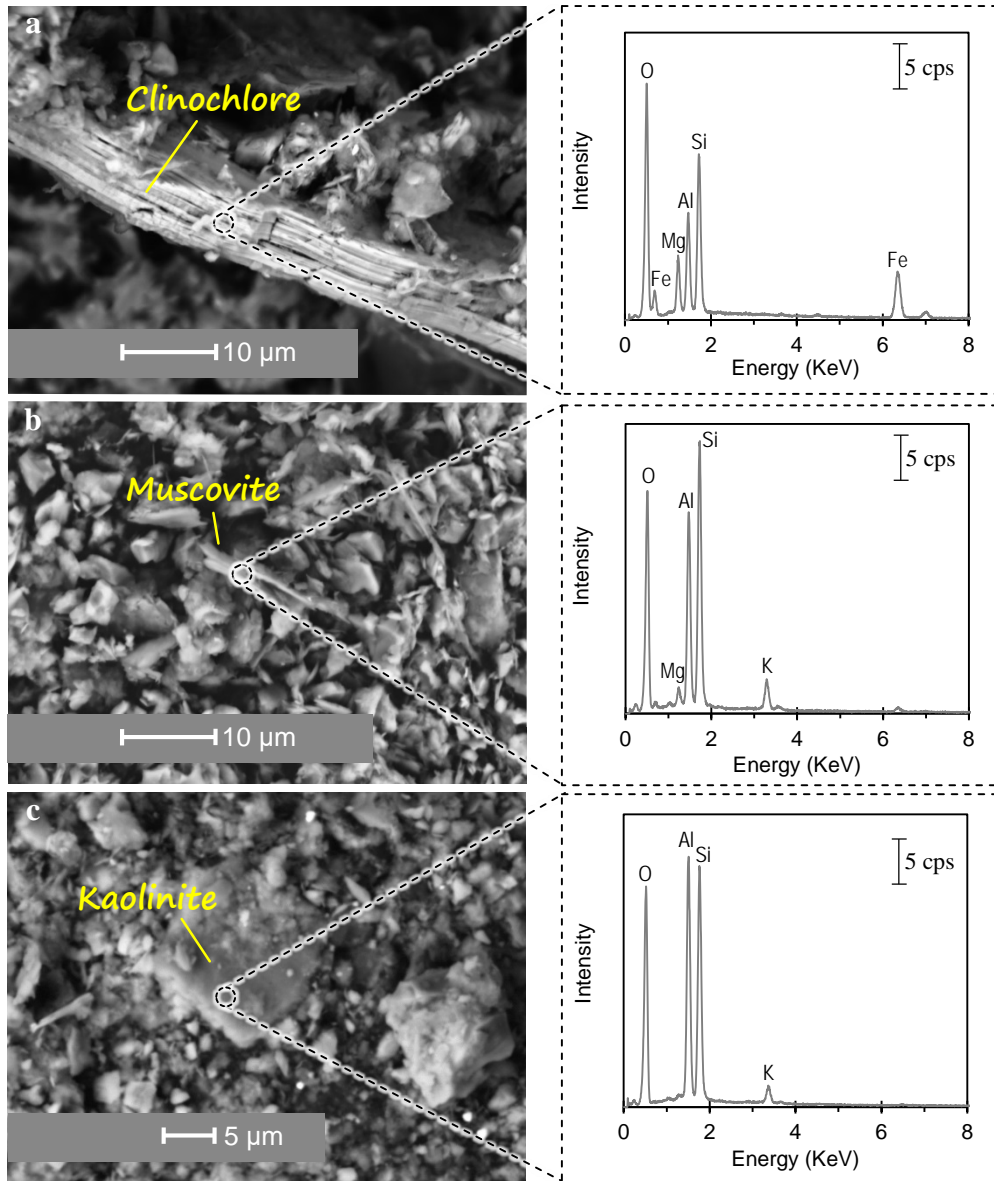


Figure 3

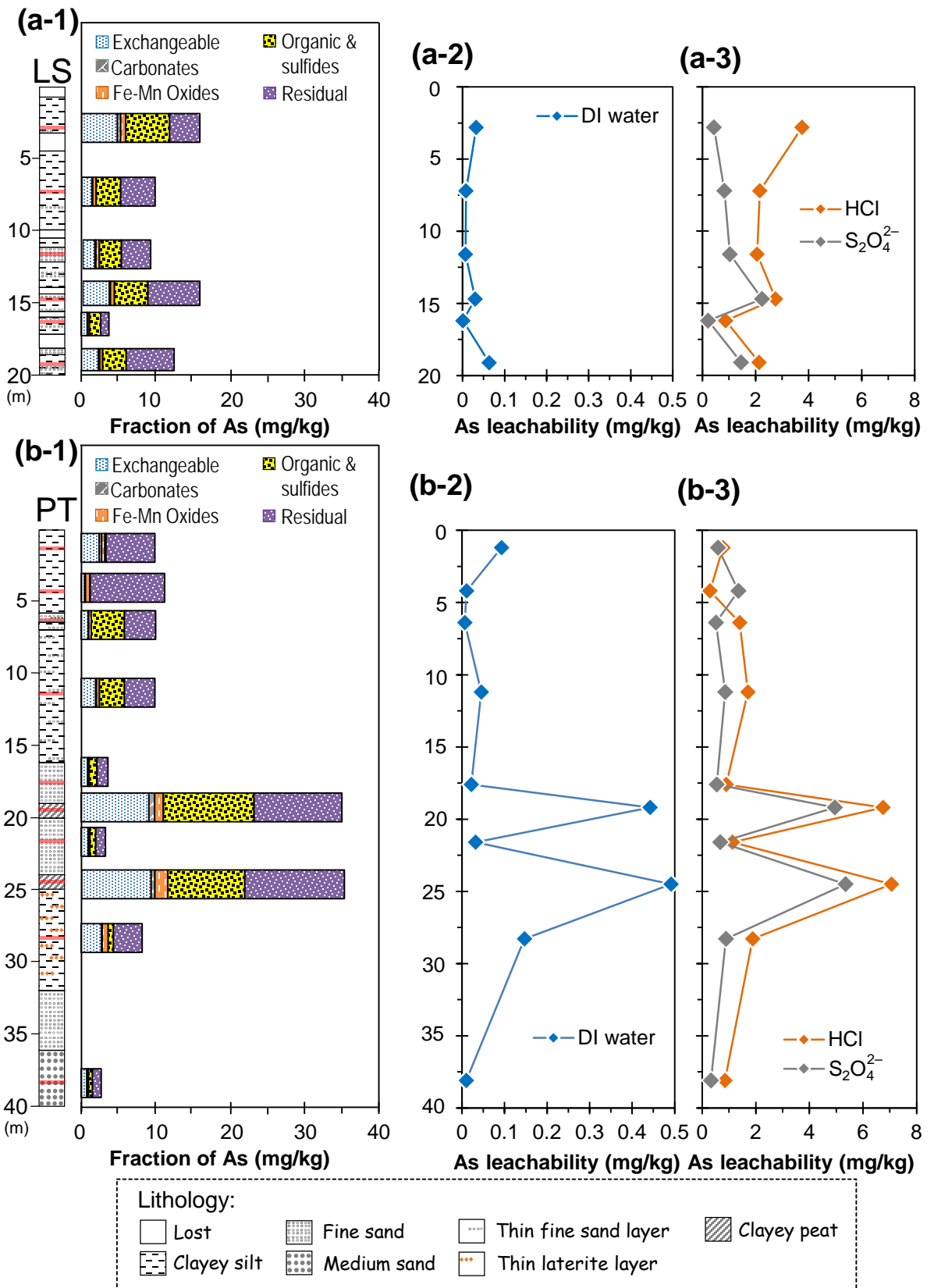


Figure 4

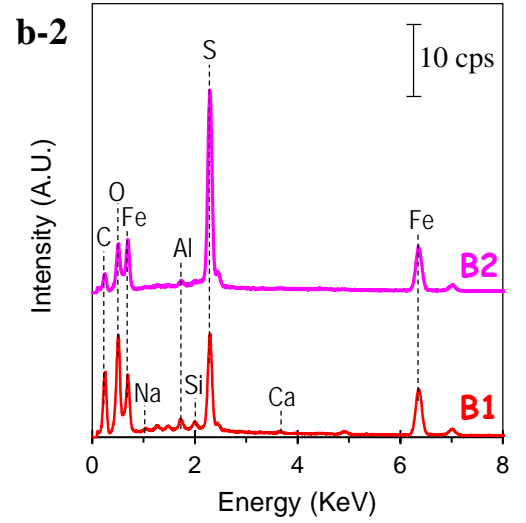
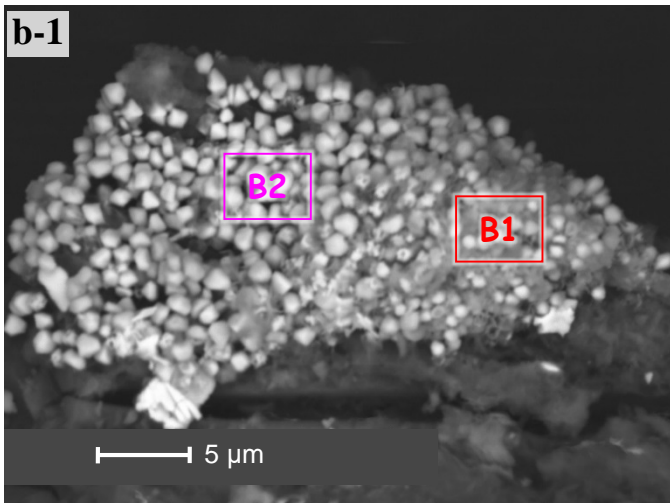
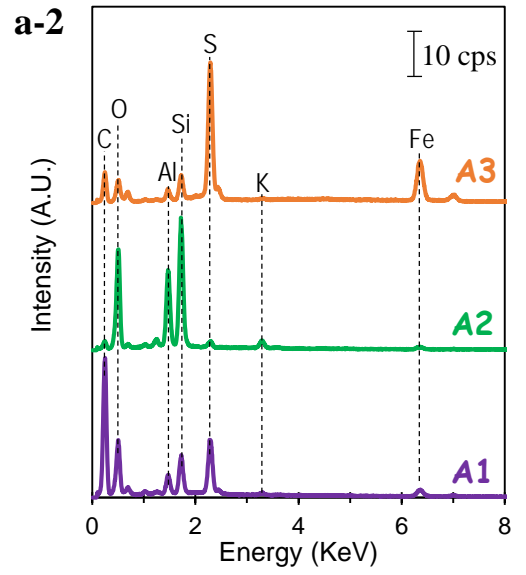
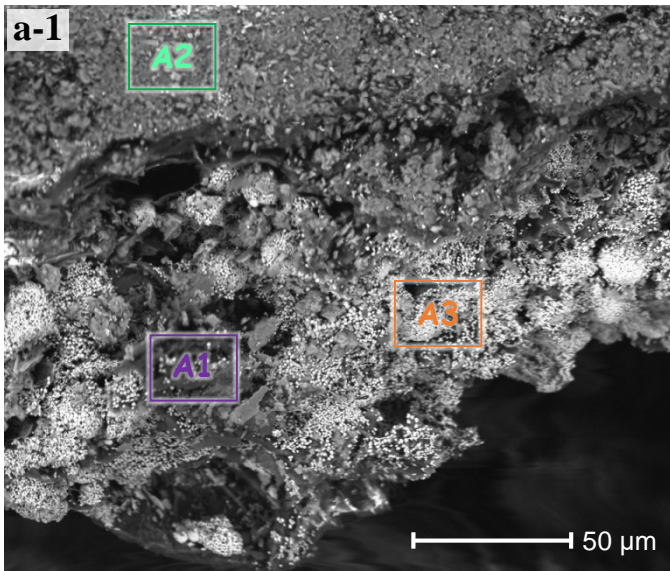


Figure 5

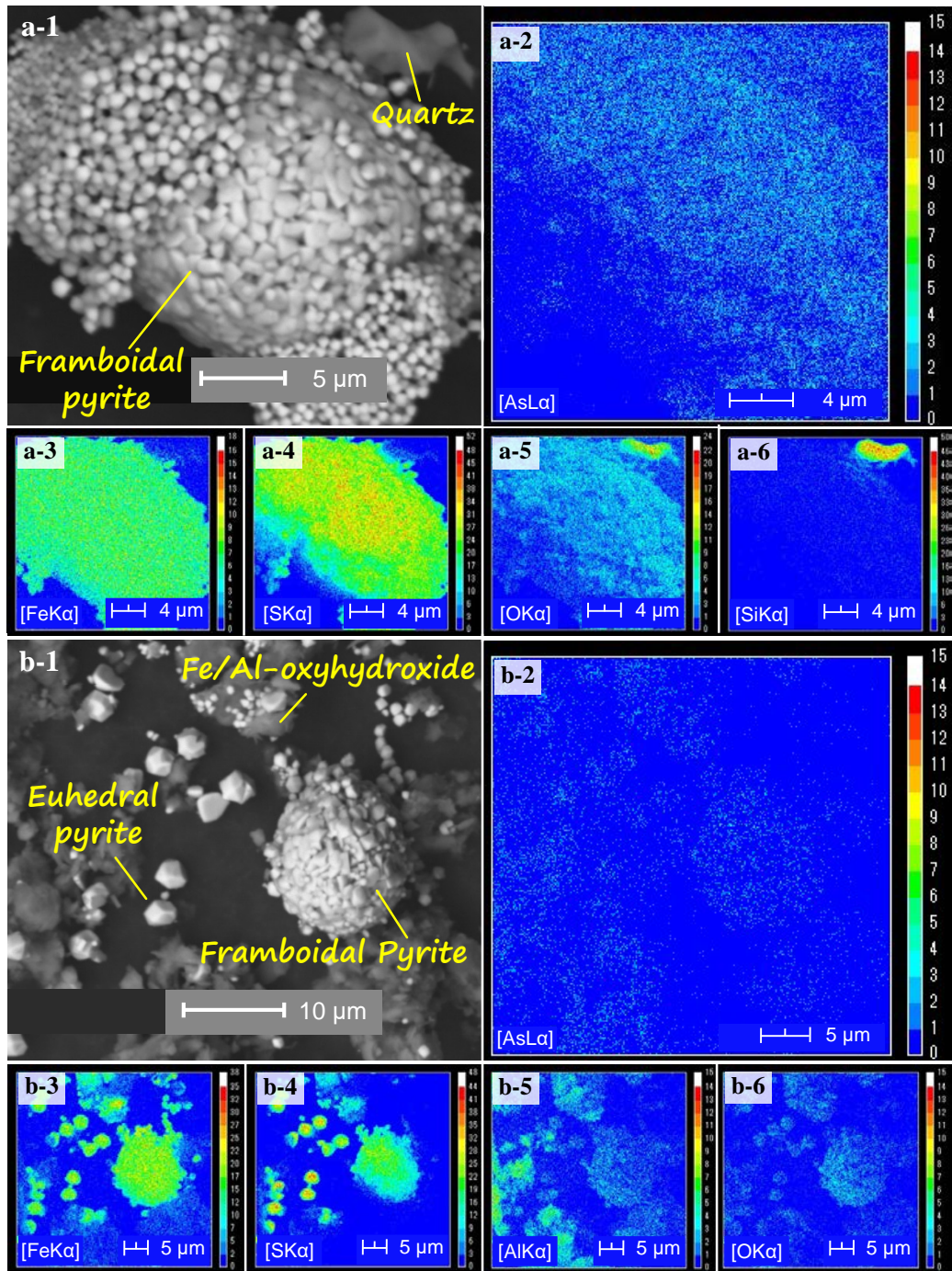


Figure 6

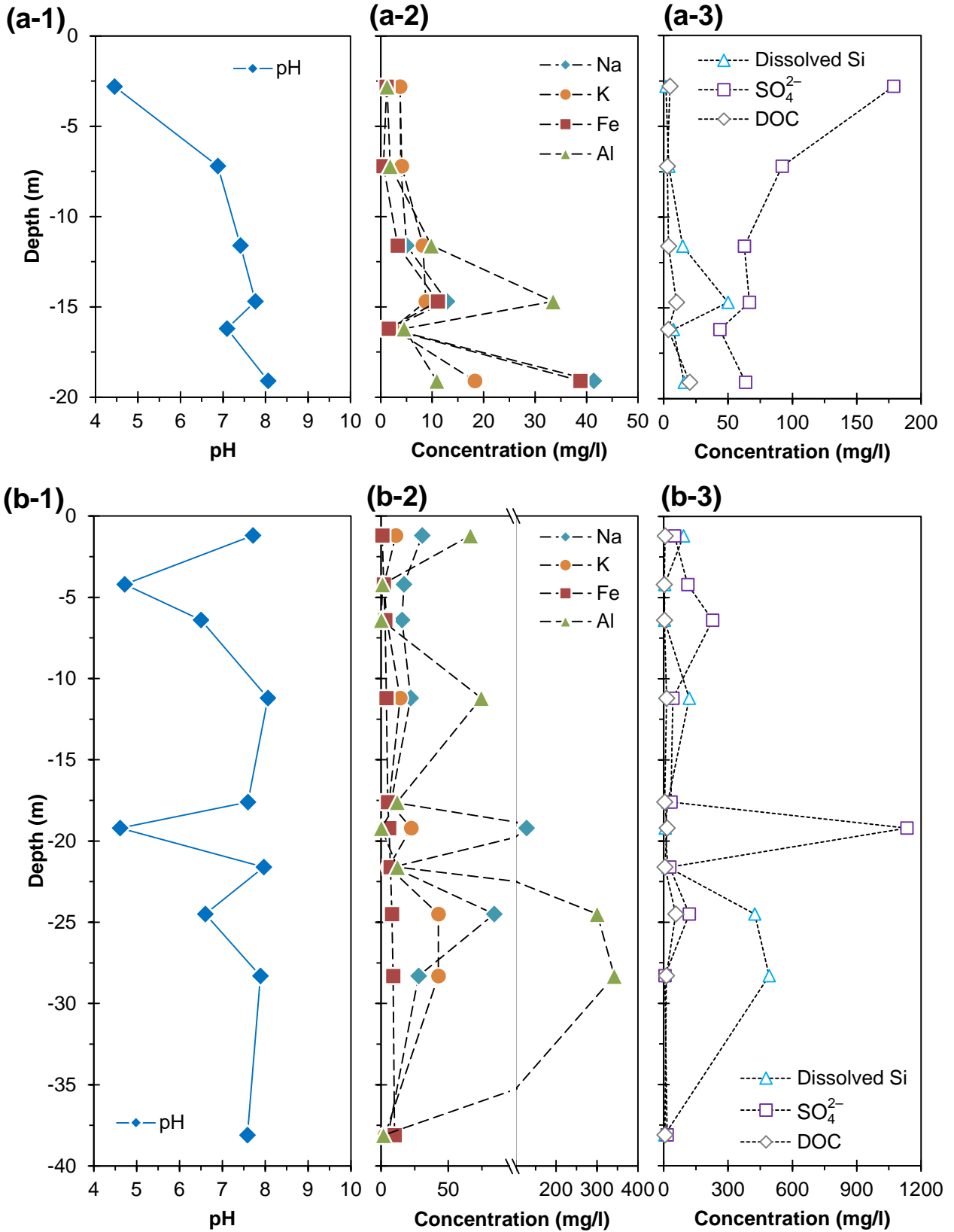


Figure 7